BRAZILIAN JOURNAL OF PETROLEUM AND GAS
Journal Homepage: www.portalabpg.org.br/bjpg
A publication of the ABPG
BRAZILIAN ASSOCIATION OF R&D IN PETROLEUM AND GAS

CFD SIMULATION OF MULTIPHASE FLOW IN A SIEVE TRAY OF A DISTILLATION COLUMN

[a] Teleken, J. G.; [a] Werle, L. O. [1]; [a] Marangoni, C.; [a] Quadri, M. B.; Machado, R. A. F.

[a]Federal University of Santa Catarina- Department of Chemical Engineering - Laboratory of Control of Processes - Technological Center

ABSTRACT

Many studies on distillation columns are based on macroscopic models of mass and energy conservation. In this work, we investigate the complex hydrodynamics of sieve trays in pilot plant distillation columns, based on a distributed control system with heating action at intermediate points, by means of electrical resistance heaters arranged on the surface of sieve trays **(Marangoni and Machado, 2007; Werle, 2007)**, using computational fluid dynamics. The main objective was to evaluate the influence of the electrical resistance heaters on the hydrodynamics of the sieve trays. A three-dimensional mathematical homogeneous biphasic model was implemented in the commercial code of computational fluid dynamics (CFD), CFX 11 (AEA Technology) for numerical experimentation studies. The results show the influence of electrical resistance heaters placed on the sieve trays on the flow patterns, although the hydrodynamics is not affected as a whole. Consequently, this helped to provide enhanced mixing and homogenization in the region with active bubbles, and thus the use of electrical resistance heaters could be applied in a distributed control system approach.

KEYWORDS

distillation columns; fluid dynamics model; CFX

[1] To whom all correspondence should be addressed.

Address: Federal University of Santa Catarina- Department of Chemical Engineering - Laboratory of Control of Processes - Technological Center - University Campus - Trindade. P.O. Box 476. ZIP Code:. Florianópolis - SC. Brazil

CEP: 88040-970 | Telephone / fax number: +55 48 3721 9554 | E-mail: leandro@enq.ufsc.br

1. INTRODUCTION

The petroleum industry is one of the greatest driving sources of technological advances in the world. This is due to the high degree of competitiveness associated with petroleum, leading to the exhaustive search for new technologies that enable greater efficiency in the related processes.

The development of sophisticated chemical processes is associated with this globalized and competitive activity, with the application of mathematical models that enable a better description of their real behavior. The process most widely used in this sector is distillation and, in this context, detailed knowledge of the mechanisms that occur is very important, particularly with regard to the sophistication of the equipment and processes **(Li et al., 2009)**.

Valve trays are widely used as phase-contact devices in distillation columns. The description of the hydrodynamics of valve trays is of great importance in industrial practice, since the separation efficiency and overall tray performance is predicted for a given set of operating conditions, tray geometries and system properties. The hydrodynamics of valve trays has been reported in many publications **(Kister, 1992; Szulczewska et al., 2003)**. However, the correlations reported for tray hydrodynamics have been largely empirical.

In recent years, there has been considerable academic and industrial interest in the use of computational fluid dynamics (CFD) to model two-phase flows in some chemical engineering equipment. The volume-of-fluid (VOF) technique can be used for prior determination of multiphase flow over structure packing. **Szulczewska et al. (2003)** simulated gas-liquid counter-current flow over a plate-type structured packing. **Gu et al. (2004)** developed a two-phase flow CFD model using the VOF method to predict the hydrodynamics of falling film flow over structured packing. **Ataki and Bart (2006)** simulated the liquid flow structure for a structured packing element and liquid redistribution at the node of the structure packing with the VOF model. There have also been many attempts to simulate sieve tray hydrodynamics using CFD. **Yu et al. (1998)** and **Liu et al. (2000)** neglected the variations in the direction of gas flow along the height of the dispersion to simulate the two-phase flow behavior, and only the hydrodynamics of the liquid flow was obtained. The inter-phase momentum exchange (drag) coefficient was required to model the hydrodynamics of multiphase flow on sieve trays. **Fischer and Quarini (1998)** attempted to describe the three-dimensional transient gas-liquid hydrodynamics, by assuming a constant drag coefficient of 0.44, which was appropriate for uniform bubble flow. This drag coefficient was not appropriate for description of the hydrodynamics of sieve trays operating in either the froth or spray regimes. **Krishna et al. (1999)** and **van Batten and Krishna (2000)** described the hydrodynamics of sieve trays by estimating a new drag correlation coefficient for a swarm of large bubbles on the basis of the correlation of **Bennett et al. (1983)** for the liquid hold-up. Because this correlation over-predicted the liquid hold-up fraction in the froth regime, **Gesit et al. (2003)** used the liquid hold-up correlation of **Colwell (1979)**, which worked well in the froth regime, to predict the flow patterns and hydraulics of commercial-scale sieve trays (CFD simulation of hydrodynamics of valve tray). There are several studies in the literature using fluid dynamics modeling for distillation columns, most notably the research by **Li et al. (2009)**, **Nikou and Ehsani, (2008)**, and **Noriler et al. (2007)**, who, in most cases, investigated the behavior of the speed vectors and the distribution of the kinetic energy of liquid-gas flows in sieve trays. The model was solved using the finite volume method with variables located in a system of generalized coordinates **(Maliska, 2004)**.

Although CFD is becoming a powerful research and design tool in chemical engineering there are no reports of simulating the hydrodynamics of valve trays using CFD. The main difficulty associated with this is that the valve floats as the valve hole gas velocity changes. When the velocity of the gas passing through the valve hole is higher than a certain value (the critical valve hole velocity), the valve is fully open. This means that the valve lifts to the maximum extent and does not float. Under this condition, CFD can be used to simulate the hydrodynamics of valve trays. In this paper, a three-dimensional transient CFD model was developed within the two-phase Euler framework for the hydrodynamics of a cylindrical fully-open valve tray. Simulations were carried out varying the superficial gas velocity, liquid weir

loads and weir heights when the valves are fully open. The objectives were: to propose the development, implementation and application of a microscopic model for momentum conservation subjected to the turbulent flow of the vapor phase; to represent the fluid dynamics of the vapor-liquid flow in a perforated plate distillation pilot plant, with validation through correlation with the experimental data provided in **Bennett et al. (1983)**; and, finally, to examine the influence of electrical resistance heaters placed on the tray surfaces to control the distributed heating of a distillation pilot plant on the fluid flow dynamics.

2. MATHEMATICAL MODEL

The model considers the gas and liquid flows in a Eulerian-Eulerian framework, where the phases are treated with transport equations. The equations used were: mass continuity and momentum equations. To solve these, it was necessary to add and use the equation of momentum flux **(Liu et al., 2000)**. It was considered that the fluctuations (turbulence) reflect the formation and dispersion of small swarms of bubbles, and that the Reynolds stresses can be linearly related to the mean velocity gradients (eddy viscosity hypothesis), as in the case of the relationship between the stress and strain tensors in laminar Newtonian flow. The standard k-ε turbulence model for multiphase flow was assumed **(Nikou and Ehsani, 2008)**.

2.1 Mass Continuity Equations

Equation 1 expresses the overall mass continuity equation.

$$\frac{\partial}{\partial t}(f_k\rho_k)+\nabla\times(f_k\rho_k v_k)=0 \quad (1)$$

where f_k, ρ_k and v_k represent the volume fraction, macroscopic density and velocity vector for the k phase, respectively. The gas and liquid volume fractions, f_g and f_l, are related through the summation constraint indicated by Equation 2:

$$f_g+f_l=1 \quad (2)$$

2.2 Momentum Equation

Equation 3 expresses the overall momentum equation.

$$\frac{\partial}{\partial t}(f_k\rho_k v_k)+\nabla\times(f_k\rho_k v_k v_k)=-f_k\nabla P_k + \\ +\nabla\times\left[f_k\mu_k\left(\nabla v_k+\nabla v_k^T\right)+M_{g.l}+f_k\rho_k g\right] \quad (3)$$

where μ_k and g represent the molecular viscosity for the k^{th} phase and the gravity vector, respectively. P_k is the pressure field, having the same value for the gas end and the liquid phase. $M_{g,l}$ represents the momentum transfer between the gas and the liquid phases, and the additional momentum flux due to the velocity fluctuation (turbulence) was incorporated into the diffusion term.

To solve Equations 1-3, an additional equation relating the interphase momentum transfer ($M_{g,l}$) and additional momentum fluxes is required, and this is provided by Equation 4.

$$M_{g,l}=\frac{3}{4}\frac{f_g\rho_l}{d_g}C_D\left|v_g-v_l\right|\left(v_g-v_l\right) \quad (4)$$

where dg is the bubble diameter and CD is the drag coefficient.

2.3 Turbulence Equations

When applying the time average procedure in the Navier Stokes equations, an extra term appears due to the turbulent fluctuation of the velocities, which needs to be represented by a constitutive equation. This term is known as the Reynolds flux. We consider that the fluctuations (turbulence) reflects the formation and dispersion of small swarms of bubbles, and that the Reynolds stresses can be linearly related to the mean velocity gradients (eddy viscosity hypothesis) as in the relationship between the stress and strain tensors in laminar Newtonian flow, and thus an effective viscosity can be assumed (Equation 5), and the Reynolds fluxes of a scalar are linearly related to the mean scalar gradient.

$$\mu_{eff}=\mu+\mu_t \quad (5)$$

The standard k-ε model is related to the turbulent kinetic energy and its dissipation rate as follows:

$$\mu^t = C_\mu \rho \left(\frac{k^2}{\varepsilon} \right) \tag{6}$$

where k is the turbulent kinetic energy and ε is the dissipation rate of the turbulent kinetic energy. The conservation equation for turbulent kinetic energy and its dissipation rate can be written as:

$$\frac{\partial}{\partial t}(r_\alpha \rho_\alpha k_\alpha) + \nabla \bullet \left(r_\alpha \left(\rho_\alpha U_\alpha k_\alpha - \left(\mu + \frac{\mu_{t\alpha}}{\sigma_k} \right) \nabla k_\alpha \right) \right) = r_\alpha (P_\alpha - \rho_\alpha \varepsilon_\alpha) + T_{\alpha\beta}^{(k)} \tag{7}$$

$$\frac{\partial}{\partial t}(r_\alpha \rho_\alpha \varepsilon_\alpha) + \nabla \bullet \left(r_\alpha \rho_\alpha U_\alpha \varepsilon_\alpha - \left(\mu + \frac{\mu_{t\alpha}}{\sigma_{\varepsilon 1}} \right) \nabla \varepsilon_\alpha \right) = r_\alpha \frac{\varepsilon_\alpha}{k_\alpha} (C_{\varepsilon 1} P_\alpha - C_{\varepsilon 2} \rho_\alpha \varepsilon_\alpha) + T_{\alpha\beta}^{(\varepsilon)} \tag{8}$$

where $C_{\varepsilon 1}$, $C_{\varepsilon 2}$, C_μ, σ_k and $\sigma_{\varepsilon 1}$ are the model constants and $T_{\alpha\beta}^{(k)}$ and $T_{\alpha\beta}^{(\varepsilon)}$ are coefficients of mass transfer between phases.

A commercial CFD package, known as CFX 11, produced by AEA Technology, was used to solve the continuity and momentum equations for the two-fluid mixture. This package is a finite volume solver, using body-fitted grids. The grid used is non-staggered and discretization of the equations at the grid is performed using a finite difference (finite volume) method.

In Figure 1 two perforated sieve trays of a distillation column are illustrated, which were studied in the CFD simulations.

2.4 Boundary and Initial Conditions

The physical space is mapped in a cylindrical computational space and boundary conditions are required for all boundaries of the physical domain. At the inlet a uniform profile of the velocities and turbulent properties is imposed, without any slip conditions on the wall for both phases. Pressure conditions at the outlet were also applied for the two phases. Figure 2 shows the physical domain used in the simulations and the configuration of the systems which were simulated. The diameter of the tray is 0.21 m with a height of 0.15 m. The length of the weir is 0.16 m and the diameter of the resistor is 0.01 m. The liquid enters the tray through a half moon-shaped opening. The number of elements in each of the numerical meshes was 415164 and 1129497 elements, respectively, for the systems without and with the presence of the electrical resistance on the surface of the plate.

Velocity vector equations are treated as scalar equations, one scalar equation for each velocity component. All scalar variables are discretized and evaluated at the cell centers. Velocities required at the cell faces are evaluated by applying an improved Rhie–Chow interpolation algorithm (Rhie and Chow, 1983). Transport variables such as diffusion coefficients and effective viscosities are evaluated and stored at the cell faces. The pressure–velocity coupling is obtained using the SIMPLEC algorithm (Van Doormal and Raithby, 1984). No problems with numerical diffusion are anticipated in view of the small size of the grid and the time steps used. A fully-implicit backward

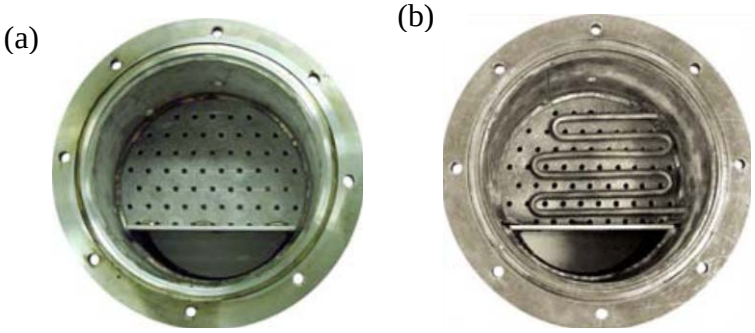

Figure 1. Top views of modules showing the characteristics of the plate (a) without and (b) with electrical resistor.

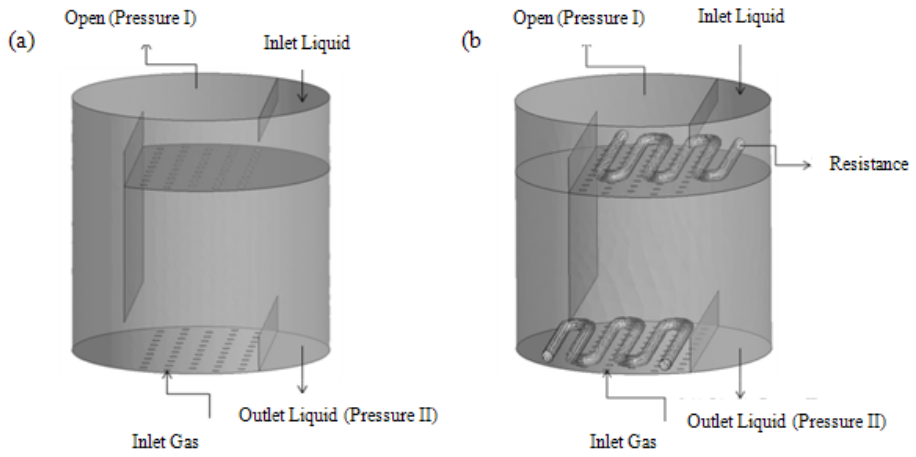

Figure 2. 3-D multiphase physical domain (a) without and (b) with electrical resistance.

difference scheme was used for the time integration.

Air, at ambient pressure, and water were used as the gas and liquid phases, respectively. At the beginning of the simulation, the conditions consisted of liquid up to the weir height, and air up to the weir height, at a homogeneous temperature equal to T_0. The velocity fields and the turbulent properties, also considered as initial conditions for each simulation, are shown in the next section. The time increment used in the simulations is 0.001 s. During the simulation the volume fraction of the liquid phase in the gas–liquid dispersion in the system is monitored and quasi-steady state is assumed to prevail if the value of the hold-up remains constant for sufficiently long period of time in order to determine the time-averaged values of the various parameters. Typically, steady state is achieved in about 12 s from the start of the simulations. Simulations were performed in a cluster with ten Pentium-4 computers with processors running at 200 MHz. A typical simulation took around 7 days to simulate 20 s of tray hydrodynamics.

3. RESULTS AND DISCUSSION

In this section, the results of simulations performed using the two physical domains studied and analyzed, that is, with and without the presence of electrical resistance on the tray surfaces, are presented.

Figures 3a and 3c show the distribution profiles of the volumetric fraction of water in the XY plane and XZ plane, respectively, at three different heights (1.5, 9.0 and 16.5 cm), without the presence of the electrical resistance on the surface of the trays. Figures 3b and 3d show the behavior of velocity vectors for air (in the XY plane) and liquid (in the XZ plane 1.5 cm above the surface), respectively.

It can be observed in Figure 3a that the retained liquid layer (hold-up) represented by the dark blue color (volume fraction of liquid equal to one) undergoes a small increase, with the mixing of both phases and foam formation because of the high gas flow.

The rising of the liquid is more pronounced in the region near the wall of the exit from the lower tray, since air inlet through the holes is a control condition with constant velocity and normal boundary, which forces the evolution of some preferential routes, such as those observed, causing part of the air to rise through the tube of the liquid drop.

Figure 3b shows the behavior of the velocity vectors of the gas phase in the XY plane. It can be observed that there are regions of large recirculation and turbulence near the walls. It is also possible to observe the appearance of some route preferences with higher gas phase velocity, as in the region near the fall barrier of the hold-up and also near the wall of the liquid drop. This confirms the behavior noted through observation of the distribution of the volume fraction of the liquid in this plane.

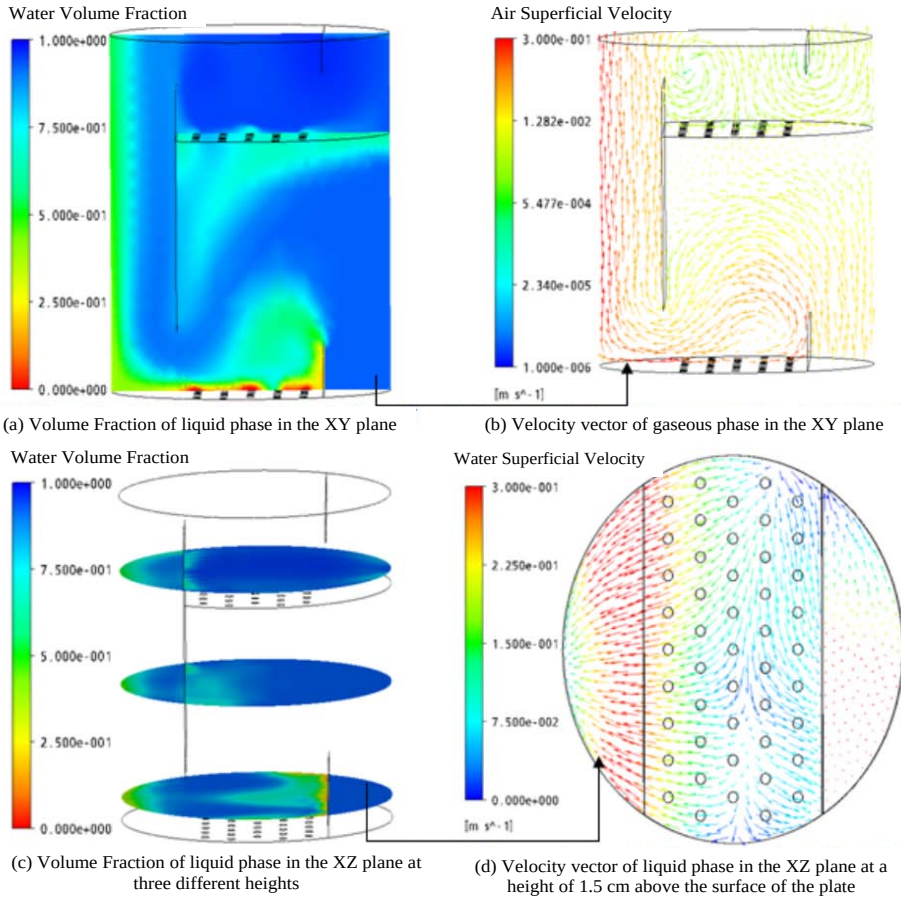

(a) Volume Fraction of liquid phase in the XY plane

(b) Velocity vector of gaseous phase in the XY plane

(c) Volume Fraction of liquid phase in the XZ plane at three different heights

(d) Velocity vector of liquid phase in the XZ plane at a height of 1.5 cm above the surface of the plate

Figure 3. Distribution of the liquid volumetric fraction and velocity vectors for multiphase flow without the electrical resistance.

Figure 3c confirms the distribution of the liquid volume fraction at three different levels in the XZ plane. It can be observed that the liquid phase distribution at 1.5 cm above the tray represents a less homogeneous mixture of liquid and vapor phases, with a region of greater concentration of air close to the hold-up fall barrier and near the wall of the liquid fall represented by the color green. This probably occurred due to the initial condition at the boundary imposed on the gas entrance flow, which is constant and normal.

The distribution of the liquid volume fraction at 1.5 cm above the top plate shows greater homogeneity of the mixture, due to the behavior of the vapor flow being closer to reality, that is, in the holes of the top plate no air entry condition was imposed because the air that passes through the liquid retained in the lower tray is the same as that which enters the holes of the top tray. The behavior of the velocity vector of the liquid phase at 1.5 cm from the surface of the plate can be observed in Figure 3d.

The presence of some circulation regions near the walls of the plate and also at the proximities of the liquid fall tube can be noted. This distillation tray behavior presents some operational and efficiency problems, but it should be noted that this study is focused on the hydrodynamics of the plate in order to study these phenomena in particular.

To demonstrate the volume fraction distribution of the liquid in the active bubbling region (-0.5 to 0.5 in X[m]), three lines were drawn on it (one in the center of the plate and two 5 cm away to the right and to the left of the central line) for both the lower tray and the top tray.

It can be observed in Figure 4 that the distribution of the liquid volume fraction in the lower tray has a large variation in the bubbling region, with points of minimum fluid concentration closer to the wall than in the case of the hold-up (close to 0.05 m). This is an undesirable factor in terms of tray operation since there will be concentration and temperature gradients on the

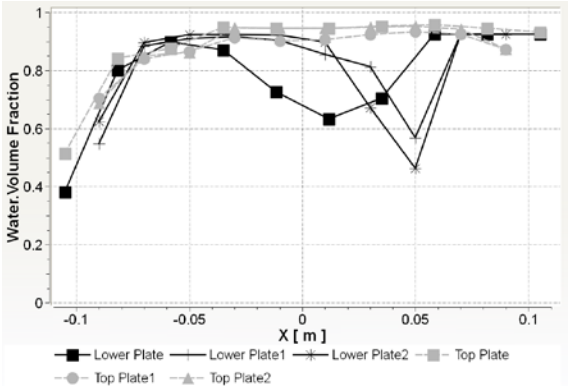

Figure 4. Volumetric fraction distribution of the liquid surface of the plates in three different areas on the surface of the tray.

surface of the tray reducing its efficiency. In the top tray phase mixture is considerably more homogeneous, which is more appropriate for the good operation of a perforated tray distillation.

The height values for the clear liquid phases were obtained in a time period which ensured the condition of a quasi-stationary state, determined through the average volumetric fraction of the liquid times the height of the computational domain. These values are shown in Figure 5 and compared with those obtained by Bennett et al. (1983) using an experimental correlation.

It can be observed in Figure 5 that there is a small difference between the values found for the clear liquid height through simulation and those obtained by Bennett et al. (1983) through experimental correlation. The 3D homogeneous multiphase model showed a behavior that was very similar to the experimental correlation of Bennett, and the results obtained with the homogeneous model predict the clear liquid height in a

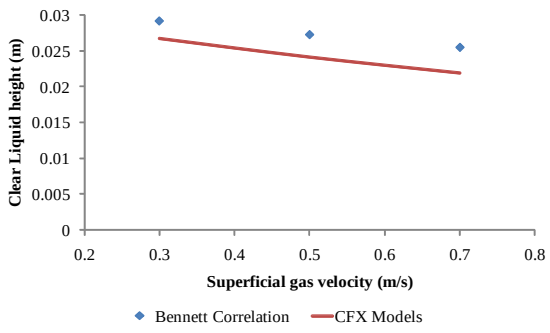

Figure 5. Comparison of the 3-D model with the correlation of Bennett et al. (1983) for the clear liquid height with a feed water velocity of 0.1 (m/s).

perforated distillation plate with an average error of 11.25%.

In order to evaluate the influence of electrical resistance on the surface of the plate on the hydrodynamics, new simulations were performed using the air and liquid flows described in the previous case as the new physical domain and the results are represented in Figure 6.

Figure 6a shows the distribution of the liquid volume fraction and illustrates again the formation of a preferential route for the gas movement for the whole liquid drop. However, in the active bubbling area the mixing occurred in a more homogeneous way with lower elevation of the hold-up. In Figure 6b, the behavior of the velocity vectors of the gas phase is observed, in the same plane for which the profile of the liquid volume fraction was demonstrated, showing circulation zones near the walls. Again it is possible to observe a preferential route for the gas phase drainage through the liquid fall tube.

In Figure 6c, it can be observed that at 1.5 cm above the surface of the lower plate the mixture of phases is not homogeneous for the plate with electrical resistance because there are points with different concentrations of water (or gas), as indicated by the presence of regions with higher concentrations of water (strong blue) and regions where water is almost absent (green tending toward red). In this situation, mass transfer does not occur in a maximized way in the bubbling region, and there are concentration gradients in this region. However, by comparing Figures 3c and 6c, it is clear that the mixing on the surface of the plates with resistance is more effective than in the case without resistance. Figure 6d shows the behavior of the velocity vectors of the liquid phase at 1.5 cm above the surface of the lower plate, where it is possible to observe that circulation occurs near the curved walls of the plate in the region of liquid fall and in some small areas near the electrical resistor wall.

Similarly, in order to demonstrate the distribution of the liquid volume fraction in the active bubbling region (-0.05 to 0.05 in X [m]) for the physical domain with the presence of the electrical resistance on the surface of the plate, three lines were drawn over this area (one in the center of the plate and two others at 5 cm to right

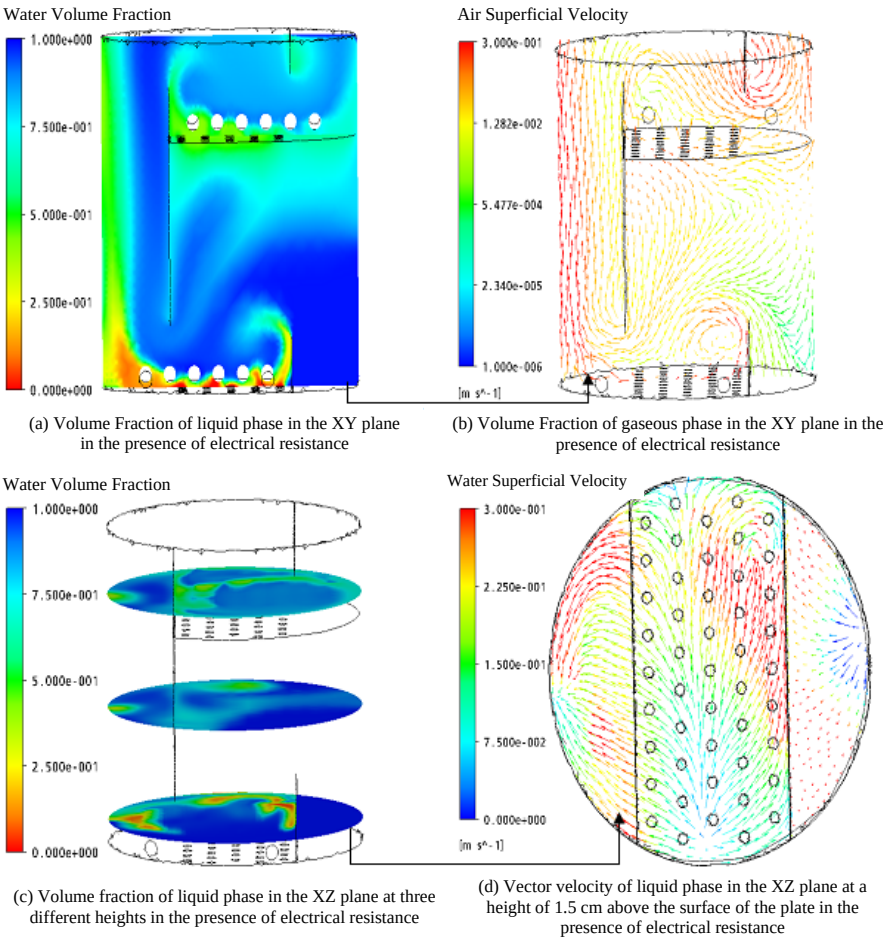

(a) Volume Fraction of liquid phase in the XY plane in the presence of electrical resistance

(b) Volume Fraction of gaseous phase in the XY plane in the presence of electrical resistance

(c) Volume fraction of liquid phase in the XZ plane at three different heights in the presence of electrical resistance

(d) Vector velocity of liquid phase in the XZ plane at a height of 1.5 cm above the surface of the plate in the presence of electrical resistance

Figure 7. Distribution of the liquid volumetric fraction and velocity vectors for multiphase flow in the presence of electrical resistance.

and left of the center line) for both the lower and upper plates.

In Figure 7, the distribution of the liquid volume fraction in the lower plate shows only a small region within which there is a considerable variation in the volume fraction of the liquid phase in the bubbling region next to the wall (hold-up, close to 0.05 m). On the top plate the mixture between the phases was considerably more homogeneous and thus satisfactory in terms of proper operation of a perforated plate distillation.

Comparing the results obtained with and without the presence of the electrical resistance on the surface of the plates, the distribution of the liquid volume fraction or, in other words, the hydrodynamic flow on the plate, was not found to be adversely affected. Analysis of Figures 4 and 7 shows that the presence of electrical resistance even favors the mixing since there is a more homogeneous distribution of the liquid volume fraction on the plate. From the separation process point of view, this is beneficial because it minimizes the possible concentration and temperature gradients in this region.

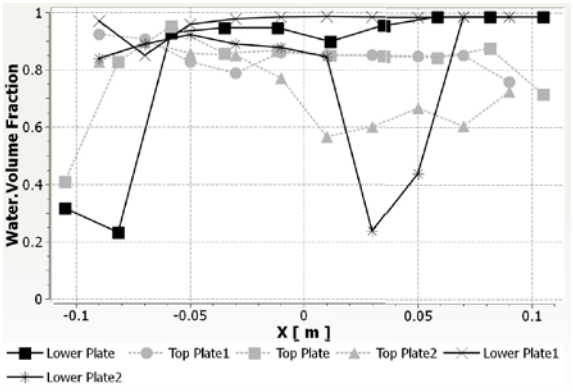

Figure 6. Distribution of the volumetric fraction of the liquid surface of the plates in three different areas on the surface of the plate in the presence of electrical resistance.

4. CONCLUSIONS

It can be concluded from the results obtained in this work that the presence of electrical resistors on the surface of the plates influences the patterns of liquid flow over them, and this does not adversely affect the hydrodynamics. In fact, it favors the homogenization of phases, indicating that the application of this methodology to control systems with distributed heating is thus a feasible option. Moreover, it improves the homogenization of phase mixing in the active bubbling region, which is very important in terms of maximizing mass transfer. From these results, future studies will be carried out with mixtures of ethanol and water in order to analyze the efficiency of the separation process of the two domains, and also to evaluate the effect of electrical resistance on the mass transfer process in this unit.

ACKNOWLEDGMENTS

The authors are grateful for financial support from the National Agency of Petroleum (ANP), and the Studies and Projects Fund (FINEP), by means of the Human Resources Program of ANP for the Petroleum and Gas sector – PRH-34-ANP/MCT.

5. REFERENCES

ATAKI, A.; BART, H. J. Experimental and CFD simulation study for the wetting of a structured packing element with liquids. Chemical Engineering Technology, v.29, p. 336–347, 2006.

BENNETT, D. L.; AGRAWAL, R.; COOK, P.J. New pressure drop correlation for sieve tray distillation columns. AIChE Journal, v. 29, p. 434–442, 1983.

COLWELL, C.L. Clear liquid height and forth density on sieve trays, Industrial and Engineering Chemistry Process Design and Development, v. 20, p. 298–299, 1979.

FISCHER, C.H.; QUARINI, G.L. Three-dimensional heterogeneous modeling of distillation tray hydraulics. Proceedings of the AIChE Annual Meeting, November 15–20, Miami Beach, USA, 1998.

GESIT, G.; NANDAKUMAR, K.; CHUANG, K.T. CFD modeling of flow patterns and hydraulics of commercial-scale sieve trays. AIChE Journal, v. 49, p. 910–924, 2003.

GU, F.; LIU, C.J.; YUAN, X.G.; YU, G.C. CFD simulation of liquid film flow on inclined plates. Chemical Engineering Technology, v. 27, p. 1099–1104, 2004.

KISTER, H.Z. Distillation Design, McGraw-Hill, New York, 1992.

KRISHNA, R.; vAN BATEN, J.M.; ELLENBERGER, J.; HIGLER, A.P.; TAYLOR, R. CFD simulations of sieve tray hydrodynamics. Chemical Engineering Research Design, v. 77, p. 639–646, 1999.

LI, X.G.; LIU, D. X.; XU, S. M.; LI, H. CFD simulation of hydrodynamics of valve tray. Chemical Engineering and Processing: Process Intensification, v. 48, p. 145-151, 2009.

LIU, C. J. X.; YUAN, G.; YU, K. T.; ZHU, X. J. A fluid-dynamic model for flow pattern on a distillation tray. Chemical Engineering Science, v. 55, p. 2287-2294, 2000.

MALISKA, C. R. Transferência de calor e mecânica dos fluidos computacional. Rio de Janeiro: Livros Técnicos e Científicos, 2004. (in Portuguese)

MARANGONI, C.; MACHADO, R. A. F. Distillation tower with distributed control strategy: Feed temperature loads. Chemical Engineering and Technology, v.30, p.1292-1297, 2007.

NIKOU, M. R. K.; EHSANI, M. R. Turbulence models application on CFD simulation of hydrodynamics, heat and mass transfer in a structured packing. International Communications in Heat and Mass Transfer, v. 35, p. 1211-1219, 2008.

NORILER, D.; MEIER, H. F.; BARROS, A. A. C.; WOLF MACIEL, M. R. Thermal fluid dynamics analysis of gas-liquid flow on a distillation sieve tray. Chemical Engineering Journal, doi:10.1016/j.cej.2007.03.023, 2007.

RHIE, C.M.; CHOW, W.L. Numerical study of the turbulent flow past an airfoil with trailing edge separation. AIAA Journal, v. 21, p. 1525–1532, 1983.

SZULCZEWSKA,B.; ZBICINSKI, I.; GORAK, A. Liquid flow on structured packing: CFD simulation and experimental study. Chemical Engineering Technology., v. 26, p. 580–584, 2003.

van BATEN, J.M.; KRISHNA, R. Modelling sieve tray hydraulics using computational fluid dynamics. Chemical Engineering. Journal, v. 77, p. 143–151, 2000.

VAN DOORMAL, J.; RAITHBY, G.D. Enhancement of the SIMPLE method for predicting incompressible flows. Number. Heat Transfer, v.7, p. 147–163, 1984.